scientific reports

Check for updates

OPEN

Seismic monitoring of 2020 Baghjan oil-well blowout incident in Assam, India

Santanu Baruah[1,2]✉, Shankho Niyogi[3], Abhijit Ghosh[3]✉, Davide Piccinini[4], Gilberto Saccorotti[4]✉, Alan L. Kafka[5], Danica Roth[6], Mahendra Kumar Yadava[7], Manoj K. Phukan[1], G. Narahari Sastry[1,8], Mohamed F. Abdelwahed[9], J. R. Kayal[10,11], Sausthov M. Bhattacharyya[1], Chandan Dey[1], Kimlina Gogoi[1,2], Timangshu Chetia[1], Prachurjya Borthakur[1,2], Sebastiano D'Amico[12], Nandita Dutta[13] & Sowrav Saikia[14]

Characterization of a productive oil/gas well blowout through seismological methods is relatively uncommon. In this paper, we conduct an in-depth seismic evaluation of one of the world's most significant onshore oil well blowout incidents, which occurred in 2020 at the Baghjan oil field in Assam, northeast India. We show that the blowout and related on-site activities generated distinct signals that can be distinguished by their spectral characteristics, temporal variation in geometric spreading, and sharp attenuation of daytime noise in comparison to the nighttime. A micro-earthquake potentially triggered by the blowout was also detected. Furthermore, we show how seismic data can be used to reasonably estimate blowout gas exit velocity and flame height. Our results demonstrate that a detailed characterization and spatiotemporal variation of blowout activity can be successfully captured through seismic monitoring, opening new opportunities for hazard mitigation and cost-effective disaster management for such catastrophic events.

Keywords Baghjan oil-blowout, Blowout quake, Rayleigh waves, Air-ground-coupled air waves (AGCA)

Oil well blowouts resulting in the uncontrolled release of natural gas or oil have been a well-known hazard of oil and gas exploration and production. Although the largest known blowouts have occurred offshore[1,2], the limited data available suggests that onshore wells are more prevalent and may experience higher failure rates[3], possibly due to older infrastructure and not as much oversight[4]. Davies et al. documented over 4 million onshore wells with failure rates from 2 to 75% across just nine nations with acceptably reliable data (i.e., Australia, Austria, Bahrain, Brazil, Canada, the Netherlands, Poland, UK, USA), though these numbers likely underestimate true rates due to poor reporting[3]. Onshore wells are also at higher risk than offshore wells of contaminating groundwater, surface water, and wetland ecosystems, and pose a higher direct hazard to human life[4]. As oil well infrastructure ages, the need for enhanced remote monitoring strategies is growing. Here we report a novel case study documenting, to our knowledge, the first use of passive seismic monitoring to track the characteristics of an active blowout event.

On May 27, 2020, oil well no. 5 of the Baghjan oil field (operated by Oil India Limited (OIL)) in the Tinsukia district of Assam experienced one of the most severe onshore blowouts in the world (see Fig. 1a, and Supplemental Material). The event ignited a catastrophic jet fire that raged at temperatures exceeding 1000 °C from June 9 to

[1]CSIR-North East Institute of Science and Technology, Jorhat, Assam 785006, India. [2]Academy of Scientific and Innovative Research, Ghaziabad, Uttar Pradesh 201 002, India. [3]Department of Earth and Planetary Sciences, University of California, Riverside, USA. [4]Istituto Nazionale di Geofisica e Vulcanologia - Sezione di Pisa, Via C. Battisti, Pisa, Italy. [5]Department of Earth and Environmental Sciences, Boston College, Chestnut Hill, MA 02467, USA. [6]Cooperative Institute for Research in Environmental Sciences (CIRES), University of Colorado Boulder, Boulder, USA. [7]Environment and Forest Department, Government of Assam, Guwahati, India. [8]Department of Biotechnology, Indian Institute of Technology-Hyderabad, Kandi, Telangana 502285, India. [9]Geohazards Research Centre, King Abdulaziz University, Jeddah, Saudi Arabia. [10]Formerly at Geological Survey of India, Kolkata, India. [11]National Institute of Technology-Agartala, Agartala, Tripura 799046, India. [12]Department of Geosciences, University of Malta, Msida, MSD 2080, Malta. [13]Assam State Disaster Management Authority (ASDMA), Assam Secretariate, Government of Assam, Dispur, Guwahati, Assam 781005, India. [14]Institute of Seismological Research, Government of Gujarat, Gandhinagar, Gujarat 382009, India. ✉email: santanub27@gmail.com; aghosh.earth@gmail.com; gilberto.saccorotti@ingv.it

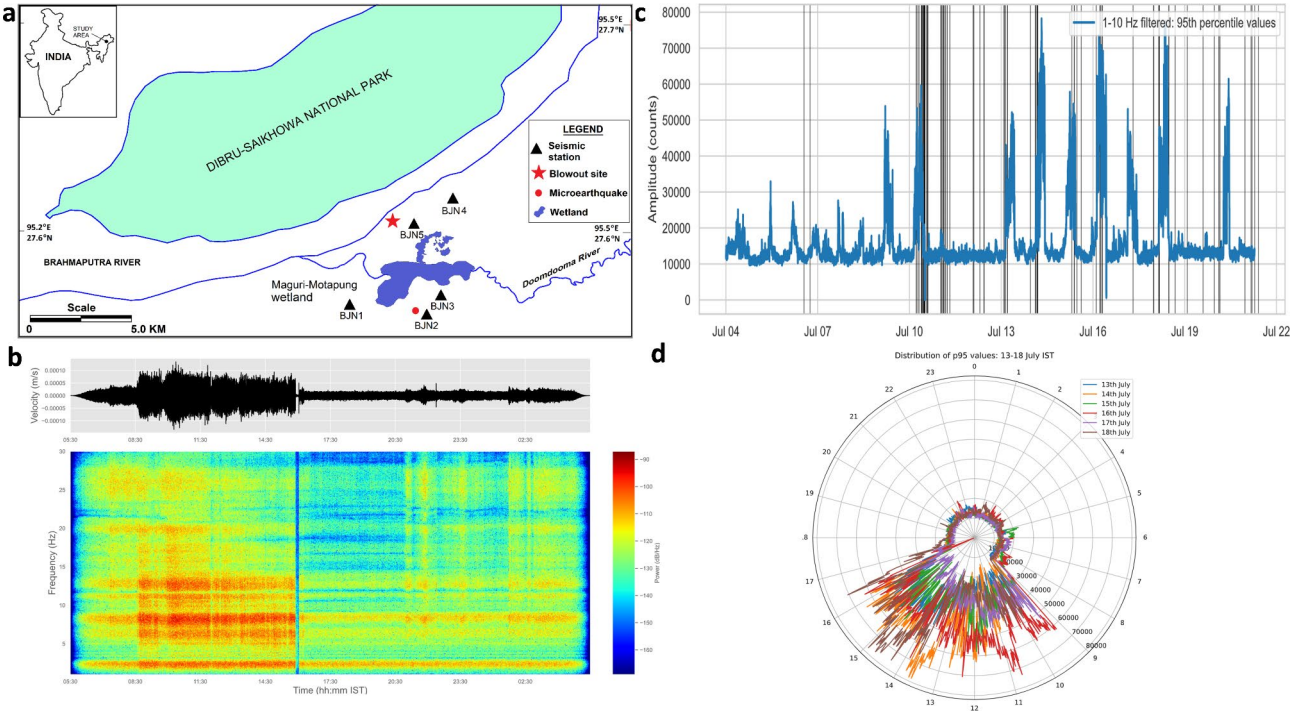

Fig. 1. Baghjan blowout study region. (**a**) Map of the study site in the Tinsukia District of Assam, India (inset) showing instrumentation and sensitive ecological zones near the blowout. (**b**) 1–30 Hz-filtered vertical ground velocity time series (top) and spectrogram (bottom) at station BJN5 over July 16, 2020. Indian Standard Time (IST). Anthropogenic noise from workers attempting to control the blowout, produces high-amplitude noise over 1–30 Hz during daytime hours, whereas the continuous gas blowout generates power primarily at 1–10 Hz, with prominent 2–3 Hz and 5–8 Hz bands persisting through nighttime hours. A brief gap in noise occurs at 15:54–16:03 IST, followed by an impulse signal explosion. (**c**) 1–10 Hz-filtered 95th percentile vertical seismic amplitude (station BJN5) shows clear diurnal variation throughout the duration of study, reflecting human activity. Gas emission and jet fire produce consistent background amplitudes; vertical grey lines mark clusters of small explosions with waveforms similar to the explosive impulse detected on July 16, 2020. (**d**) Rose diagram showing clear daily activity from ~ 8 a.m. to ~ 5 p.m. (IST) in the temporal distribution of 1–10 Hz-filtered 95th percentile amplitudes over 13–18th July, 2020. Radial distance marks seismic amplitude in counts, and numbers along the circumference indicate hours of day starting at midnight IST.

November 15, 2020, causing widespread evacuations and a few fatalities, with an estimated USD 3.2 billion of ecological damages[5]. The blowout had far-reaching consequences, not only on the environment but also on noise pollution and ground vibrations, soil and water pollution, and thermal pollution that significantly impacted the lives of the nearby communities. The fire at the blowout well, sourced by uninterrupted upwelling of natural gas and condensate at more than 4,000 psi, perpetually flamed with an average height of 108 m. The spontaneous noise produced from the well, similar to that of the sound of a jet-engine, reached more than 100 dB within 100 m radius and more than 50 dB within 5 km radius. The flames of the blowout raised the heat of both the air and water of the surrounding area by ~ 7 °C above the ambient temperature, amounting to thermal pollution.

In the aftermath of this event, it has also resulted in the loss of an estimated 55 per cent of the biodiversity in the affected Dibru-Saikhowa National Park. As many as 1,632 hectares of wetland, 523 ha of grassland, 172 ha of area covering rivers and streams, and 213 ha of forest were damaged to varying degrees based on the proximity of the ecosystem to the blowout[6]. Experts say it may take more than 10 years for even a partial recovery of the destruction caused to the landscape[7]. To the best of our knowledge, this event is one of the worst onshore blowout-fueled jet fires that has been documented in history[6] and therefore warrants multidisciplinary studies which can help in prevention and mitigation of such accidents in the future. Here, we investigate characteristics of seismo-acoustic noise, in particular "air-ground-coupled-air" waves (AGCA)[8–10] generated by the blowout, as well as related activities, captured on a temporary broadband seismic network. Our results provide new insights into blowout conditions and highlight the potential advantages of employing seismo-acoustic monitoring for remote detection and management of blowout events and related activities.

A literature review on similar events, such as explosions and gas pipeline bursts, highlights the distinctive advantages of using seismic data in studying these occurrences, offering insights that few other methods can provide. Koper et al.[11] discuss seismic recordings of a natural gas pipeline explosion in Carlsbad, New Mexico, on August 19, 2000. Their study analyzed the recorded seismic signals during which they identified three impulsive events and two extended seismic events related to the explosion and continuous emanation of the flaming gases, respectively. Their study provided insights into the nature and timing of the pipeline explosion event. The seismic

analysis was valuable for law enforcement agencies investigating this incident and for litigation processes. A related study by Stahler et al.[12] investigated recorded seismic events linked to the Nordstream pipeline subsea explosions in the Baltic Sea. They located two significant seismic events near the observed methane plumes by analyzing the polarization of seismic signals from multiple stations. This study is an example of the application of seismology in locating the explosions and thus establishing the cause of the pipeline burst, which is useful for mitigating the harmful effects of such explosions. The Barros et al.[13] study of the 2020 Beirut explosion, one of the largest non-nuclear explosions in history, employed seismic and infrasound data for their investigation. Their study estimated the explosion's epicenter, magnitudes, and explosive yield highlighting the joint analysis of seismo-acoustic signals to better understand and quantify large-scale explosions. Another study which follows a similar methodology, Evers et al.[14] investigates a gas pipeline explosion near Ghislenghien, Belgium, using seismo-acoustic methods. Their analysis used array-processing techniques and atmospheric models to determine the explosion's origin time and location and yield using data from several seismic and infrasound stations. A similar study by Schneider et al.[15] investigates the Baumgarten gas explosion in Austria using seismo-acoustic methods. The study describes the explosion's characteristics by analyzing data from seismic and infrasound stations and modeling ray paths in the atmosphere. These studies highlight the effectiveness of seismic and acoustic methods in forensic investigations of analyzing non-tectonic seismic events such as explosions, which is important to people and society.

Seismological studies of explosions, therefore provide insights for future mitigation and response strategies along with the scientific characterization of the events. The information that these studies provide, such as the precise location and timing of explosions, is useful for law enforcement and investigative agencies. These studies also help us understand the dynamics of explosions, which can help formulate safety protocols and standards customized for a specific operation or area. Therefore, integrating seismological monitoring program into safety and planning frameworks is an important component of explosion risk management.

The preliminary report on the Baghjan gas blowout by the Central Pollution Control Board, Government of India (2020) also highlights concerns regarding the seismic vulnerability of the region in the wake of the gas blowout, which motivated the seismic monitoring that forms the basis of this study. The northeastern state of Assam, India, where the gas blowout took place, is a region prone to seismic activity, having recorded many earthquakes in the past[16–19]. The continuous gas blowouts and further drilling attempts to bring it under control could also have potentially generated induced seismicity, so monitoring with local seismic stations was necessary. Fluvial floodplains and wetlands characterize the local landscape of the region, which would also have amplified ground motion in the case of any induced seismicity, making this area particularly susceptible to damage from seismic activity. The same report also highlights that constant tremor related to the gas blowout caused significant damage to the area's infrastructure, roads, and homes. These vibrations had adversely affected the local community, causing physical and mental stress, disrupting education and livelihood, and impacting the health of residents. After the blowout was subdued, seismological monitoring provided data on the intensity and frequency of these tremors that can be used for remedial and compensatory relief measures. The impact of this gas blowout was severe enough to warrant other studies using remote sensing data to study the environmental impact (Arandhara et al.[20]). Our seismological study of the event enhances the damage assessment by showcasing the extent of ground vibrations and its variations in space and time, that can affect nearby structures and ecosystems. In this case, seismological studies complement conventional environmental assessment techniques and taken together offer a more comprehensive understanding of the blowout's impact on the surrounding sensitive ecosystem.

First detection of an onshore blowout-triggered earthquake?

Earthquakes induced by oil and gas extraction activities are a known phenomenon[21–23]. Here we investigate whether earthquakes might have been induced by the Baghjan blowout. Our data showcases the first reported micro-earthquake associated with a blowout event, at a distance of about 5 km south of the well and at a depth of ~ 1.9 km (Mc 0.5, Fig. 1a). Based on a global compilation of injection well-induced earthquakes, Goebel and Brodsky[24] showed that many such earthquakes occur at distances from the well ranging from 10 m to over 10 km. The triggering mechanism of induced earthquakes are, however, not yet fully understood, and exceptions exist such as the Bakken Shale Formation in North Dakota, which has experienced little to no induced seismicity despite thousands of injection wells being in operation there[25,26]. Thus, given that we do not yet have a fully-developed understanding of a possible blowout inducing mechanism as in the injection well induced case, we can only speculate that this earthquake at ~ 5 km distance from the blowout might be what we refer to here as a "blowout quake."

If the blowout did indeed trigger this earthquake, this might represent the first recorded earthquake directly linked to a well blowout. The earthquake's shallow depth further suggests it could be an induced phenomenon. Identifying the exact cause of this "blowout quake" remains challenging, though rapid changes in subsurface pore pressure resulting from the blowout are a plausible explanation. Additionally, the shutdown of nearby wells during the blowout could have forced fluids to migrate, potentially altering the pore pressure conditions.

Type of noise

Frequency-domain analysis of the seismic data recorded in this study reveals the presence of high-energy monochromatic signals, which we interpret as stemming from human activity, such as the use of electric generators and water pumps during fire-fighting efforts. Conversely, the broad pulses detected could likely be linked to mini-explosion—sudden fluctuations in the gas jet flux emanating from the blowout well. The estimated maximum Peak Particle Velocity (PPV) was 0.22 mm/s at the nearest station (BJN5) and the minimum was 0.095 mm/s at a farther station (BJN3).

We observe a clear daily variation in seismic amplitude (Fig. 1b–d), with high noise levels lasting ~ 8 h per day during typical daytime working hours and lulls over nights and weekends, indicating that high amplitudes correspond with human activities. Because most human activity in this area throughout the study involved fire suppression at the blowout site, the majority of this noise was likely generated by a combination of fire suppression activities, continuous gas blowout and continuously operating machines such as water pumps.

Evenings and weekends are typically characterized by continuous lower levels of noise likely dominated by noise generated by uncontrolled release of gas, as well as water pumps that ran continuously throughout the study period, creating a 'water-umbrella' to manage temperatures in the blowout site[27].

At several times throughout the study period, noise levels dropped dramatically for several minutes. Outside of these quiet periods, clear amplitude peaks at 2–3 Hz and 5–8 Hz are observed at nearly all seismic stations (Fig. 1b), visible as prominent spectral stripes in a daylong spectrogram (Fig. 1b). These bands disappear during periods of reduced noise, when energy is distributed relatively evenly over 1–10 Hz. We therefore interpret the 2–3 Hz and 5–8 Hz bands as blowout-generated noise. During working hours, the noise level is elevated over broad frequency bands, typically 1–30 Hz, which we infer to be caused by people actively working and operating machines at the blowout site.

We also observe several distinct impulse signals throughout the study period. One of the clearest impulse signals was recorded on July 16, 2020 (Fig. 1b), at the end of a period of reduced noise. Vertical and radial component seismograms of this pulse show relatively high energy with little energy on the transverse component (Fig. 2a). Particle motion also shows elliptical motion in the vertical-radial plane (Fig. 2b) suggesting that the pulse is composed of Rayleigh waves. Spectral characteristics of the pulse match the 2–3 and 5–8 Hz bands found during times of active gas blowout, suggesting that the noise produced by the gas blowout is also dominated by Rayleigh waves (Fig. 2c).

We use this impulsive mini-explosion signal as a template and apply a match filter technique to identify similar pulses during the 17-day study period. Such impulse signals typically occur in clusters and are observed sporadically throughout the duration studied here, both at day and night times, suggesting they are likely smaller explosions producing weak pulses of AGCA Rayleigh waves.

It is important to note that the frequency bands can vary depending on the individual characteristics of the blowout event and the surrounding geological environment. In this case, the blowout site is located at soft alluvium where the predominant frequency of the site is lower, thus the appearance of prominent spectral stripes

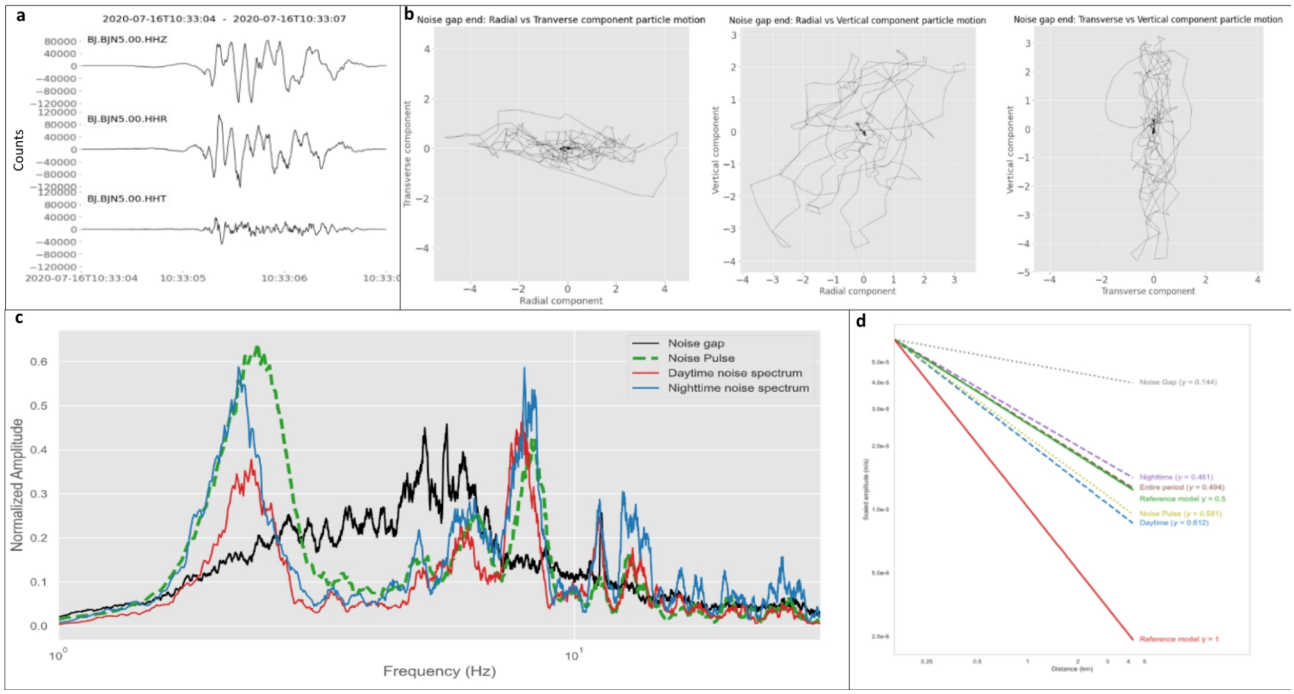

Fig. 2. Key characteristics of distinct signals. (**a**) Impulse signal of an explosion detected July 16, 2020 (station BJN5). (**b**) Particle motion associated with the impulse signal occurs primarily in the vertical and radial directions, indicative of a Rayleigh wave. (**c**) Normalized example spectra for vertical motion associated with each type of signal discussed in the text. Daytime noise, nighttime noise and July 16 explosion impulse contain peaks at 2–3 Hz and 5–8 Hz, suggesting that power in these bands is generated by related processes associated with the blowout; the relatively lower amplitude of daytime spectral peaks reflects the addition of broadband anthropogenic noise. The noise gap and the micro-earthquake on July 5 demonstrate unique spectral characteristics, suggesting distinct sources. (**d**) Decay in seismic amplitude with distance from the blowout and estimated geometric attenuation coefficient γ for each type of signal (see Materials and Methods for details). Theoretical models for attenuation in pure surface waves (γ = 0.5) and body waves (γ = 1) shown for reference.

at lower frequencies. Had it been a rocky site, the predominant frequency of the site could have been higher, thus influencing the prominent spectral stripes. A more comprehensive analysis, including additional data (e.g., recording of background seismic noise after controlling the blowout at the same locations where recording was done during blowout) and modeling, would be necessary to provide a definitive explanation for the observed frequency bands.

Noise attenuation

We use the blowout as the assumed source of noise and determine its seismic attenuation, which we attribute to be mostly geometrical spreading, and its diurnal variation. Near the source, geometrical spreading is the dominant factor that determines how ground shaking decays with distance[28]. Ground shaking is controlled by the source, path, and near-surface site conditions. During the study period, path and site conditions remain nearly unchanged. Thus, geometrical spreading is an important element of modeling predicted ground motion in an area[29,30]. It is typically determined by analyzing natural earthquakes data[18–20]. In this case, however, we took a novel approach of determining geometrical spreading from a coherent, near-continuous and strong noise source. Time also provides an additional dimension in this study, as the noise characteristics change throughout the day. As discussed earlier in detail, there are three types of noise recorded here. Here, we determine geometrical spreading separately using different types of noise occurring in different time periods and compare them.

Surprisingly, geometrical spreading appears to vary over time in the study area, which as described below can be explained by different types of waves (body waves and surface waves) mixed in different proportions dominating the ground motion at different times (Fig. 2d; Table 1). Amplitudes of seismic surface and body waves theoretically decay at $R^{-0.5}$ and R^{-1}, respectively, where R is distance from the source. Noise in this study is dominated by the blowout, which is by far the strongest continuous source of noise in the study area. Generally, we find that the amplitude of noise in the study area decays at a rate close to $R^{-0.5}$ indicating that the wavefield is dominated by surface waves (Fig. 2d) as suggested by previous analyses of the impulse signal. Surface waves from the blowout are the main source of noise during nighttime periods ($R^{-0.46}$). Daytime amplitude decay consistently shows steeper slopes($R^{-0.61}$) compared to nighttime even though the amplitude is higher compared to nighttime (Fig. 2d). We can conceive of no mechanistic reason for surface wave amplitudes to decay faster with distance during the day, and therefore infer that the apparent increase in decay rate results from the near-field signal being a combination of body waves produced by human activities during the day superposed on surface waves from the blowout.

The impulse signal detected on July 16, 2020 occurred during daytime at around 16:00 h (IST) and decays at a rate of $R^{-0.581}$, suggesting that higher amplitude surface waves from the impulse are reducing the relative dominance of daytime anthropogenic body waves. This observation supports our conclusion that the impulse is likely a result of small explosion during blowout. We have performed this analysis over various frequency ranges spanning 1 to 30 Hz. The highest concentration of energy is observed below 10 Hz, although considerable energy can be seen up to 30 Hz as well. Increasing frequency from 10 Hz to 30 Hz, however, does not change the decay slope significantly, implying that even at higher frequencies surface waves dominate the wavefield (Fig. 2d). This is because inelastic attenuation is nonlinear and higher frequencies decay with distance at a faster rate. We thus conclude that, geometrical spreading is likely the controlling factor for amplitude decay at this distance.

Notably, the decay rate during one of the short periods of reduced noise is almost flat suggesting no strong coherent source of noise active in the area during this calm period. This suggests that more localized noise dominates the wavefield around each seismometer during these times, supporting our conclusion that the calm periods reflect short pauses or significant reductions of the blowout. This is a reasonable interpretation considering that crews were trying to plug the blowout during this time.

Source characterization

The arrival times of the pulse that occurred on July 16, 2020 could be precisely picked at different stations of the network (Fig. 3a). Joint inversion of these arrival times for source location and propagation velocity indicates acoustic waves that originated from a source located at the blowout site. (Fig. 3b,c). The continuous background noise exhibits the largest coherence over the 1–3 Hz frequency band (Fig. 4a), which corresponds to the stationary vibrations also observed in the daylong spectrograms of Fig. 1b. Coherency analysis is utilized to derive accurate estimates of differential travel times between stations. The inversion of these times reveals a stationary source location, which coincides with the blowout site. The amplitude of the signal exhibits a characteristic daily pattern, likely reflecting the disturbances generated by the fire extinguishing operations (Fig. 4b), as described in previous sections in detail. The composite location map shown in Fig. 4c exhibits a pronounced peak at the blowout site, with average discrepancies of approximately 50 m and 150 m along the east-west (EW) and north-

	1–10 Hz	2–6 Hz	2–10 Hz	1–30 Hz
Pulse	0.58	0.54	0.60	0.53
Daytime	0.61	0.54	0.67	0.59
Nighttime	0.46	0.38	0.55	0.43
Calm	0.14	0.2	0.15	− 0.31

Table 1. Geometrical spreading at different frequency bands; numbers show value of γ, the exponent of R in $1/R^{\gamma}$.

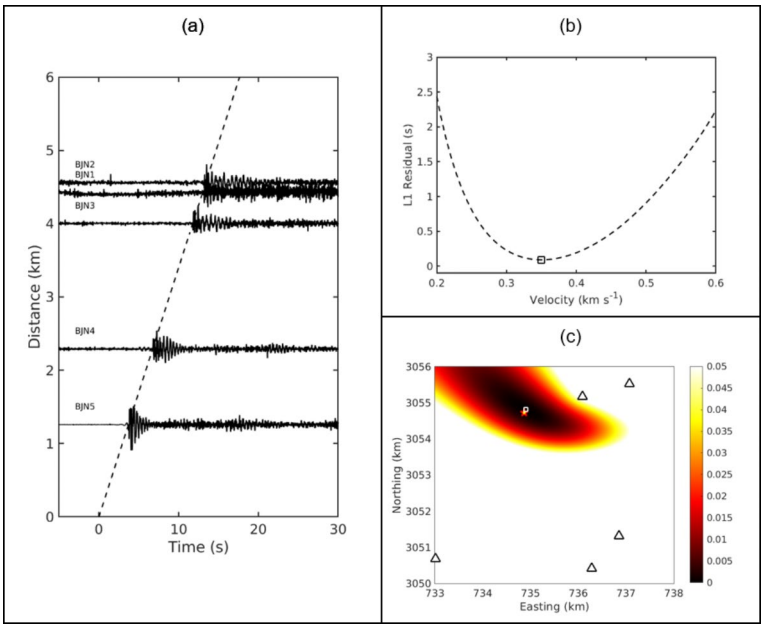

Fig. 3. (**a**) Vertical-component seismograms for the explosion impulse observed on July 16, 2020, at 16:03 IST. Data are plotted at increasing distance from the blowout location. (**b**) RMS of L1-norm location residuals for different trail velocities. The minimum residual is associated with a propagation velocity of 350 m s^{-1}. (**c**) Map of the L1 error function for source location. The square marks the minimum of this function, which corresponds to the best estimate of source location. The star indicates the location of the blowout. Coordinates are in the UTM-WGS84 projection.

south (NS) directions, respectively. These discrepancies arise due to deviations from the assumptions of constant sound velocity and a static atmosphere, which we initially adopted for predicting travel times.

Estimating jet characteristics

Our analyses suggest that the blowout generated AGCA Rayleigh waves which are acoustic waves that impinge on the Earth's surface and generate (i.e., couple to the ground as) seismic surface waves[31–33]. Similar signals are frequently produced by volcanic eruptions so acoustic infrasound recordings have been extensively utilized in monitoring and surveillance of active volcanoes to detect eruptions in remote locations, measure eruptive parameters, and infer eruption source processes[34,35]. The acoustic power radiated during gaseous volcanic eruptions has been shown to correlate positively with gas exit velocity, in turn exhibiting a positive correlation with ash plume height. We apply this theory described for volcanic jet aeroacoustics[36] to the gas explosion of the Baghjan blowout. Assuming that the ground motion is linked to AGCA waves, we use seismic recordings from each station to estimate the infrasonic acoustic pressure at the source. As a result, we obtain estimates for the gas exit velocity, which is approximately 1260 m/s, and the flame height, which is approximately 97 m. (See *Methods*, in *Supplementary Material* for a complete description of this analysis.). Despite the use of several simplifying assumptions in this approach (Methods), these model results are remarkably consistent with field-reported values of ~ 1000 m/s and ~ 100 m, respectively (Table 2 in Supplementary Material)[6].

Conclusions

In this study, we analyzed continuous recordings of seismic noise collected by a temporary seismic network installed within a 10 km radius of the Baghjan well blowout site for a total duration of 17 days. Our analysis documents details of the characteristics of seismic data recorded in the vicinity of the blowout, and also documents what we conclude to be the first known case of a blowout microearthquake. This documentation contributes to a growing database and understanding of how seismological analysis elucidates the phenomenon of oil and gas well blowout accidents. Further investigation of past and future seismic data recorded in the vicinity of blowouts will help determine whether such events are common, and could contribute to our growing knowledge of the mechanics and mitigation strategies for these types of oil and gas well explosion accidents, as well as for other environmental hazards associated with oil and natural gas producing facilities, such as the well-known conundrum of injection-induced earthquakes.

The precise source locations and detailed source property characteristics obtained in this study indicate that densely distributed permanent or temporary seismic networks can effectively supplement existing, but sparsely located, infrasound arrays. This approach provides valuable information for identifying and locating infrasonic blowout sources at both local and regional scales. Several lines of evidence suggest that sustained ground vibrations observed in the 2–3 Hz and 5–8 Hz bands are likely associated with the propagation of blowout-generated acoustic waves dynamically coupled to the ground as Rayleigh waves. Our estimates of gas jet velocity

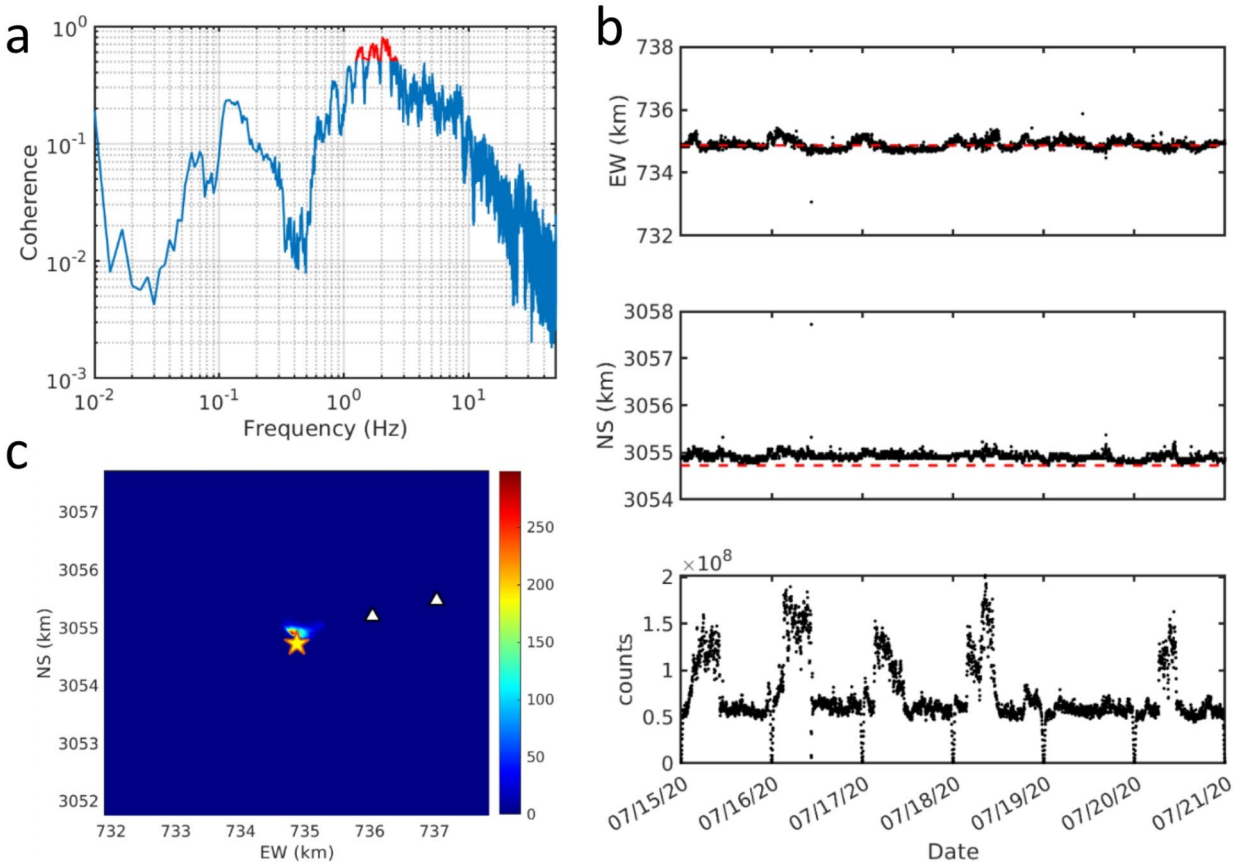

Fig. 4. (**a**) Multichannel coherence for 1-day-long recording of seismic noise at the vertical components of the Baghjan network, derived by averaging the magnitude-squared coherence functions evaluated at all independent station pairs. The frequency band within which the coherence is greater than 0.5 is highlighted in red. (**b**) Results from the grid search noise location. The top two plots show the time evolution of the source coordinates along the EW and NS directions. The bottom plot shows the RMS amplitude of the signal, as observed at the closest station. The sharp decays of signal amplitude which are observed every 24 h are due to tapering of the daily data streams. Red dashed lines indicate the blowout site position. (**c**) Frequency distribution (2-D histogram) of source location derived from the EDT inversion of noise data. Colors indicate the number of observations in 50 × 50 m bins, according to the color scale at the right. The yellow star marks the location of the blowout well. Coordinates are in UTM-WGS84 projection.

and flame height obtained from acoustic power suggest that seismic instruments could provide a real-time tool to inform emergency response personnel regarding pragmatic intervention through quantitative monitoring of such events. Our detection of explosion clustering also suggests the potential for future development of seismic early warning systems to improve safety measures for disaster response crews.

To the best of our knowledge, no studies have previously documented seismic signals during an active and continuous blowout of an oil/gas well. However, dense seismic arrays are currently used in several oil producing countries for monitoring the activity of producing oil and gas wells[37,38], providing a convenient pathway to adapt existing resources for emergency monitoring. This work thus paves the way to a vast array of seismological applications for the rapid assessment and ongoing monitoring of hazardous phenomena.

Data availability

The raw seismic Data can be provided with a request to the Director, CSIR-NEIST Jorhat at director@neist.res.in via Gmail Drive. The link of the Gmail drive is https://drive.google.com/drive/folders/1c8n1ckVUbcbzp7F-HM68BqJFNDxyu7BHy in main manuscript.

Received: 30 November 2023; Accepted: 26 September 2024
Published online: 15 October 2024

References

1. Danenberger, E. P. Outer continental shelf drilling blowouts, 1971–1991. In *All Days* OTC-7248-MS (OTC, 1993). https://doi.org/10.4043/7248-MS.

2. Hickman, S. H. et al. Scientific basis for safely shutting in the Macondo Well after the April 20, 2010 *Deepwater Horizon* blowout. *Proc. Natl. Acad. Sci.* **109**, 20268–20273 (2012).
3. Davies, R. J. et al. Oil and gas wells and their integrity: Implications for shale and unconventional resource exploitation. *Mar. Pet. Geol.* **56**, 239–254 (2014).
4. King, G. E. & King, D. E. Environmental risk arising from well-construction failure—Differences between barrier and well failure, and estimates of failure frequency across common well types, locations, and well age. *SPE Prod. Oper.* **28**, 323–344 (2013).
5. Swaddle, T. & Naraharisetty, R. Biodiversity loss due to Assam's Baghjan oil disaster could take decades to recover: Report. *The Swaddle*. https://theswaddle.com/biodiversity-loss-due-to-assams-baghjan-oil-disaster-could-take-decades-to-recover-report/ (2021).
6. Yadava, M. K. *One Man Enquiry Committee Report on Damages to Environment, Biodiversity, Wildlife, Forest and Ecology on account of Blow out and Explosion at OIL Well No. BGN-5, Baghjan, Tinsukia, Assam, India,* vol. I, 512 http://webservers.amtron.in/demo/baghjan/ (2021).
7. Ghosh, R. G. & Ghosh, S. In Assam, biodiversity loss due to the Baghjan oil blowout could take at least a decade to recover. *Scroll. in*. https://scroll.in/article/999437/in-assam-biodiversity-loss-due-to-the-baghjan-oil-blowout-could-take-at-least-a-decade-to-recover (2021).
8. Fee, D. et al. Seismic envelope-based detection and location of ground-coupled airwaves from volcanoes in Alaska. *Bull. Seismol. Soc. Am.* **106**, 1024–1035 (2016).
9. Ichihara, M., Yamakawa, K. & Muramatsu, D. A simple method to evaluate the air-to-ground coupling efficiency: A tool helping the assessment of seismic/infrasonic energy partitioning during an eruption. *Earth Planets Space* **73**, 180 (2021).
10. Bishop, J. W., Fee, D., Modrak, R., Tape, C. & Kim, K. Spectral element modeling of acoustic to seismic coupling over topography. *J. Geophys. Res. Solid Earth* **127**, e2021JB023142 (2022).
11. Koper, K. D., Wallace, T. C. & Aster, R. C. Seismic recordings of the Carlsbad, New Mexico, pipeline explosion of 19 August 2000. *Bull. Seismol. Soc. Am.* **93**(4), 1427–1432 (2003).
12. Stähler, S. C., Zenhäusern, G., Clinton, J., & Giardini, D. Locating the Nordstream explosions without a velocity model using polarization analysis. arXiv preprint https://arxiv.org/abs/2210.04585 (2022).
13. Barros, L. V. et al. Seismo-acoustic signal analysis and yield estimate of the Beirut, Lebanon, accidental explosion on August 4, 2020. *Brazilian Journal of Geophysics* **39**(4), 629–644 (2021).
14. Evers, L. G., Ceranna, L., Haak, H. W., Le Pichon, A. & Whitaker, R. W. A seismoacoustic analysis of the gas-pipeline explosion near Ghislenghien in Belgium. *Bull. Seismol. Soc. Am.* **97**(2), 417–425 (2007).
15. Schneider, F. M. et al. Seismo-acoustic signals of the Baumgarten (Austria) gas explosion detected by the AlpArray seismic network. *Earth Planet. Sci. Lett.* **502**, 104–114 (2018).
16. Ben-Menahem, A., Aboodi, E. & Schild, R. The source of the great Assam earthquake—an interplate wedge motion. *Phys. Earth Planet. Interiors* **9**(4), 265–289 (1974).
17. England, P. & Bilham, R. The Shillong Plateau and the great 1897 Assam earthquake. *Tectonics* **34**(9), 1792–1812 (2015).
18. Kayal, J. R. et al. Large and great earthquakes in the Shillong plateau–Assam valley area of Northeast India Region: Pop-up and transverse tectonics. *Tectonophysics* **532**, 186–192 (2012).
19. Khattri, K. N. Great earthquakes, seismicity gaps and potential for earthquake disaster along the Himalaya plate boundary. *Tectonophysics* **138**(1), 79–92 (1987).
20. Arandhara, B., Shukla, J. & Dhyani, S. Damage assessment of Baghjan oil field blowout on terrestrial and aquatic ecosystems near Dibru Saikhowa Biosphere Reserve, Assam India. *Remote Sens. Appl. Soc. Environ.* **31**, 100999 (2023).
21. Ellsworth, W. L. Injection-induced earthquakes. *Science* **341**, 1225942 (2013).
22. Keranen, K. M., Weingarten, M., Abers, G. A., Bekins, B. A. & Ge, S. Sharp increase in central Oklahoma seismicity since 2008 induced by massive wastewater injection. *Science* **345**, 448–451 (2014).
23. Guglielmi, Y., Cappa, F., Avouac, J.-P., Henry, P. & Elsworth, D. Seismicity triggered by fluid injection–induced aseismic slip. *Science* **348**, 1224–1226 (2015).
24. Goebel, T. H. W. & Brodsky, E. E. The spatial footprint of injection wells in a global compilation of induced earthquake sequences. *Science* **361**, 899–904 (2018).
25. Weingarten, M., Ge, S., Godt, J. W., Bekins, B. A. & Rubinstein, J. L. High-rate injection is associated with the increase in U.S. mid-continent seismicity. *Science* **348**, 1336–1340 (2015).
26. Verdon, J. P., Kendall, J.-M., Horleston, A. C. & Stork, A. L. Subsurface fluid injection and induced seismicity in southeast Saskatchewan. *Int. J. Greenh. Gas Control* **54**, 429–440 (2016).
27. Das, G. *After Big Blowout, Assam's Baghjan Oil Field Catches Fire*. https://thewire.in/environment/assam-tinsukia-baghjan-oil-field-blowout-catches-fire.
28. Wu, Q., Chapman, M. C., Beale, J. N. & Shamsalsadati, S. Near-source geometrical spreading in the central Virginia seismic zone determined from the aftershocks of the 2011 mineral, Virginia, earthquake. *Bull. Seismol. Soc. Am.* **106**, 943–955 (2016).
29. Frankel, A. Decay of *S*-wave amplitudes with distance for earthquakes in the Charlevoix, Quebec, Area: Effects of radiation pattern and directivity. *Bull. Seismol. Soc. Am.* **105**, 850–857 (2015).
30. Sedaghati, F. & Pezeshk, S. Estimation of the coda-wave attenuation and geometrical spreading in the New Madrid seismic zone. *Bull. Seismol. Soc. Am.* **106**, 1482–1498 (2016).
31. Donn, W. L., Pfeffer, R. L. & Ewing, M. Propagation of air waves from nuclear explosions: Nuclear explosions provide data on the relation of air-wave propagation to atmospheric structure. *Science* **139**, 307–317 (1963).
32. Bolt, B. A. Seismic air waves from the great 1964 Alaskan earthquake. *Nature* **202**, 1095–1096 (1964).
33. Arrowsmith, S. J., Johnson, J. B., Drob, D. P. & Hedlin, M. A. H. The seismoacoustic wavefield: a new paradigm in studying geophysical phenomena. *Rev. Geophys.* **48**, RG4003 (2010).
34. Donn, W. L. & Balachandran, N. K. Mount St. Helens Eruption of 18 May 1980: Air waves and explosive yield. *Science* **213**, 539–541 (1981).
35. Morrissey, M. M. & Chouet, B. A. Burst conditions of explosive volcanic eruptions recorded on microbarographs. *Science* **275**, 1290–1293 (1997).
36. Matoza, R. S., Fee, D., Neilsen, T. B., Gee, K. L. & Ogden, D. E. Aeroacoustics of volcanic jets: Acoustic power estimation and jet velocity dependence: Volcanic jet aeroacoustics. *J. Geophys. Res. Solid Earth* **118**, 6269–6284 (2013).
37. Das, I. & Zoback, M. D. Long-period, long-duration seismic events during hydraulic stimulation of shale and tight-gas reservoirs—Part 1: Waveform characteristics. *Geophysics* **78**, KS97–KS108 (2013).
38. Hu, H., Li, A. & Zavala-Torres, R. Long-period long-duration seismic events during hydraulic fracturing: Implications for tensile fracture development. *Geophys. Res. Lett.* **44**, 4814–4819 (2017).

Acknowledgements

We thank Government of Assam for help rendered during execution of the project. CSIR, Govt. of India is also thankfully acknowledge for their help and necessary permission. Oil India Limited (OIL), Duliajan, Assam, India provided financial support via Ref No. OIL/CONT/LOA/G/134/2020-21; date: 24/06/2020. Thanks to all the project members for executing the project during CoVID-19 pandemic period. Special thanks to Dr. Sau-

rabh Baruah, Chief Scientist, CSIR-NEIST Jorhat and Mr. I. Baruah, OIL, Duliajan, Assam, India for their help in executing the project. We thank the anonymous reviewers and Editor for their constructive comments in improving the paper. Thanks to Dr. V. M. Tiwari, Director, CSIR-NEIST, Jorhat, Assam, India for his permission to publish this article.

Author contributions

S.B. conceptualized the work. S.B., A.G., D.P., G.S. J.R.K., C.D. wrote the original manuscript. S.B., A.L.K., D.R., S.M.B., M.F.A., S.D.A. performed the seismic analysis. S.B., A.G., S.N. and S.M.B. performed the noise analysis. D.P., G.S. performed the infrasound analysis. S.B., M.K.P., S.M.B., and C.D. performed the field surveys including data generation and collection. M.K.Y. performed various survey related to study of the flame, pollution, impact assessment and other. S.B., M.K.P., G.N.S. assisted with the project management and field work coordination. Thorough check-up of the results obtained are performed by: S.B., A.G., D.P., G.S., A.L.K., D.R., M.F.A., S.D.A. The manuscript was reviewed by S.B., A.L.K., D.R., J.R.K. and G.N.S. The manuscript has been formatted and figures have been comprehensively detailed by S.B., K.G., T.C., P.B., N.D., and S.S. All authors interpreted and discussed the final results, and edited, reviewed and approved the final manuscript.

Declarations

Competing interests

The authors declare no competing interests.

Additional information

Supplementary Information The online version contains supplementary material available at https://doi.org/10.1038/s41598-024-74428-y.

Correspondence and requests for materials should be addressed to S.B., A.G. or G.S.